

Wake-up effect in $HfHf_{0.4}Zr_{0.6}O_2$ ferroelectric thin-film capacitors under a cycling electric field

Yilin Li(李屹林), Hui Zhu(朱慧), Rui Li(李锐), Jie Liu(柳杰), Jinjuan Xiang(项金娟), Na Xie(解娜), Zeng Huang(黄增), Zhixuan Fang(方志轩), Xing Liu(刘行), and Lixing Zhou(周丽星)

Citation: Chin. Phys. B, 2022, 31 (**8**): 088502. DOI: 10.1088/1674-1056/ac5977
Journal homepage: http://cpb.iphy.ac.cn; http://iopscience.iop.org/cpb

What follows is a list of articles you may be interested in

Designing high *k* dielectric films with LiPON—Al_2O_3 hybrid structure by atomic layer deposition

Ze Feng(冯泽), Yitong Wang(王一同), Jilong Hao(郝继龙), Meiyi Jing(井美艺), Feng Lu(卢峰), Weihua Wang(王维华), Yahui Cheng(程雅慧), Shengkai Wang(王盛凯), Hui Liu(刘晖), and Hong Dong(董红)

Chin. Phys. B, 2022, 31 (**5**): 057701. DOI: 10.1088/1674-1056/ac3736

Observation of source/drain bias-controlled quantum transport spectrum in junctionless silicon nanowire transistor

Yang-Yan Guo(郭仰岩), Wei-Hua Han(韩伟华), Xiao-Di Zhang(张晓迪), Jun-Dong Chen(陈俊东), and Fu-Hua Yang(杨富华)

Chin. Phys. B, 2022, 31 (**1**): 017701. DOI: 10.1088/1674-1056/ac21ba

Defect induced room-temperature ferromagnetism and enhanced photocatalytic activity in Ni-doped ZnO synthesized by electrodeposition

Deepika, Raju Kumar, Ritesh Kumar, Kamdeo Prasad Yadav, Pratyush Vaibhav, Seema Sharma, Rakesh Kumar Singh, and Santosh Kumar†

Chin. Phys. B, 2020, 29 (**10**): 108503. DOI: 10.1088/1674-1056/ab9c0c

Variable-*K* double trenches SOI LDMOS with high-concentration P-pillar

Lijuan Wu(吴丽娟), Lin Zhu(朱琳), Xing Chen(陈星)

Chin. Phys. B, 2020, 29 (**5**): 057701. DOI: 10.1088/1674-1056/ab7e94

Tuning the phase separation in $La_{0.325}Pr_{0.3}Ca_{0.375}MnO_3$ using theelectric double-layer field effect

Cui Li-Min, Li Jie, Zhang Yu, Zhao Lu, Deng Hui, Huang Ke-Qiang, Li He-Kang, Zheng Dong-Ning

Chin. Phys. B, 2014, 23 (**9**): 098501. DOI: 10.1088/1674-1056/23/9/098501

Wake-up effect in $Hf_{0.4}Zr_{0.6}O_2$ ferroelectric thin-film capacitors under a cycling electric field

Yilin Li(李屹林)[1], Hui Zhu(朱慧)[1,†], Rui Li(李锐)[1], Jie Liu(柳杰)[1], Jinjuan Xiang(项金娟)[2], Na Xie(解娜)[1], Zeng Huang(黄增)[1], Zhixuan Fang(方志轩)[1], Xing Liu(刘行)[1], and Lixing Zhou(周丽星)[1]

[1] *Faculty of Information Technology, Beijing University of Technology, Beijing* 100023, *China*
[2] *Institute of Microelectronics, Chinese Academy of Sciences, Beijing* 100029, *China*

(Received 25 November 2021; revised manuscript received 9 February 2022; accepted manuscript online 2 March 2022)

We examined the wake-up effect in a TiN/$Hf_{0.4}Zr_{0.6}O_2$/TiN structure. The increased polarization was affected by the cumulative duration of a switched electric field and the single application time of the field during each switching cycle. The space-charge-limited current was stable, indicating that the trap density did not change during the wake-up. The effective charge density in the space-charge region was extracted from capacitance–voltage curves, which demonstrated an increase in free charges at the interface. Based on changing characteristics in these properties, the wake-up effect can be attributed to the redistribution of oxygen vacancies under the electric field.

Keywords: wake up, HZO ferroelectric thin-film, cycling electric field, oxygen vacancy

PACS: 85.50.Gk, 77.55.D,77.55.fp, 72.10.–d **DOI:** 10.1088/1674-1056/ac5977

1. Introduction

Recently, high-*k* dielectrics such as HfO_2 have been extensively implemented in the microelectronics industry. In 2011, HfO_2-SiO_2 thin films were discovered to exhibit ferroelectric properties by Böscke *et al.*[1] HfO_2 exists in the form of three basic crystal structures, which are monoclinic, tetragonal and cubic. These structures are centrosymmetric and exhibit no ferroelectric polarization.[2,3] By doping HfO_2 with Si, Zr, Y, etc., an orthorhombic phase can be obtained. The structure exhibits asymmetric centrality, which is responsible for its ferroelectric properties.[4,5] Ferroelectric random-access memories using HfO_2-based thin films exhibit fast read and write speeds (tens of ns), low operating voltages, and small power consumption. Furthermore, compared to traditional ferroelectric materials (such as PZT), HfO_2-based thin films were compatible with existing CMOS semiconductor processes. They had a sufficiently strong polarization strength (15–45 μC/cm^2) in the nanometer range (10 nm).[6–9] As a high-*k* material, the leakage current of HfO_2 was low, giving it good retention properties (about 10 years).[10] This opens a new path for the development of ferroelectric field-effect transistors.[11]

A memory device undergoes continuous writing, reading, and data updating, and thus requires a ferroelectric thin film to withstand the large number of switching cycles. This brings about reliability problems, such as the wake-up effect, which refers to the increase in remnant polarization relative to the initial state at the beginning of 10^3–10^4 switching cycles.[12] A number of wake-up mechanisms have been proposed, including an oxygen vacancy redistribution,[13] field-cycling-induced phase transitions,[14] and domain de-pinning mechanisms.[12] Oxygen vacancies play an important role because they are positively charged and are mobile at room temperature.[15,16] Under an electric field, a redistribution of oxygen vacancies ($V_{\ddot{O}}$) within the oxide can occur, which de-pins the domain walls and increases the remnant polarization.[13,17] A phase transition from the tetragonal to the ferroelectric orthorhombic phase is another factor in the wake-up effect, and can be stabilized by redistributed oxygen vacancies.[12,18] Starschich *et al.* reported that the duration of the electric field was essential for the wake-up, indicating the importance of oxygen vacancy movement driven by the field.[13] To study the parameters affecting the wake-up effect in HfO_2-based thin-film devices, and to understand the associated property changes, a deeper understanding of the mechanism is needed. Moreover, because oxygen vacancies are thought to play an important role, it is expected to provide valuable information for further discussion of the vacancy changes during the wake-up process. Here, we analyzed the wake-up behavior in the TiN/$Hf_{0.4}Zr_{0.6}O_2$/TiN structure. Various switching waveforms were applied to investigate the dependence of the wake-up effect, and the variations in the remnant polarization, current–voltage (*I*–*V*) curve, and capacitance–voltage (*C*–*V*) characteristics were analyzed. A mechanism based on oxygen vacancies is proposed.

2. Experimental methods

To prepare samples for this work, $Hf_{0.4}Zr_{0.6}O_2$ (HZO) thin films with a thickness of 10 nm were deposited on silicon substrates at 300 °C under N_2 carrier gas atmosphere by

†Corresponding author. E-mail: zhuhui@bjut.edu.cn

© 2022 Chinese Physical Society and IOP Publishing Ltd

atomic layer deposition. The deposition process used precursors of tetrakis-(ethylmethylamino)-(hafnium/zirconium) and H_2O as the oxygen source. To serve as a bottom electrode, a 10-nm-thick TiN layer was deposited on the silicon substrate by magnetron sputtering. Square TiN top electrodes, with a side width of 100 μm, were deposited on the HZO films by physical vapor deposition. To prevent the top electrode from being oxidized in air, a 75-nm-thick W electrode was DC sputtered on top of it. The TiN/HZO/TiN structures were annealed at a high temperature of 450 °C. Polarization–voltage (P–V) hysteresis loops were measured with a radiant precision workstation. I–V and C–V curves were acquired with a semiconductor parameter analyzer (Agilent Technologies B1500A). In all tests, the bottom electrode was grounded, and the top electrode was biased with a drive voltage.

3. Results and discussion

The HZO thin film was cycled with 1-kHz, ±3 V square waveforms. Changes in the P–V curves during the cycling are shown in Fig. 1(a). The initial state displayed a double hysteresis, which is a signature of anti-ferroelectric behavior.[20] After repetitive switching, it is transformed into a single ferroelectric hysteresis loop. The evolution of the remnant polarization and coercive voltage as a function of switching cycles are plotted in Figs. 1(b) and 1(c). Both the magnitude of remnant polarization (P_r) and coercive voltage (V_c) increased during the first 10^4 cycles. This was consistent with the wake-up effect in the polarization hysteresis of HZO thin films. With a further increase in the number of field cycles, the P_r and V_c decreased, which corresponded to fatigue generally observed in many ferroelectrics. In addition, the magnitude of the negative coercive voltage V_{c-} was always less than that of the positive coercive voltage V_{c+}, indicating the presence of an internal built-in electric filed in the HZO film pointing from the bottom to the top interface. We calculated the built-in voltage V_{bi} by $(V_{c+}-V_{c-})/2$[21] and plotted them as a function switching cycles in Fig. 1(c). It can be seen that the magnitude of built-in voltage stayed stable in the wake-up stage, but increased obviously after 10^4 cycles, which should contribute to the shift of P–V hysteresis loops.[31]

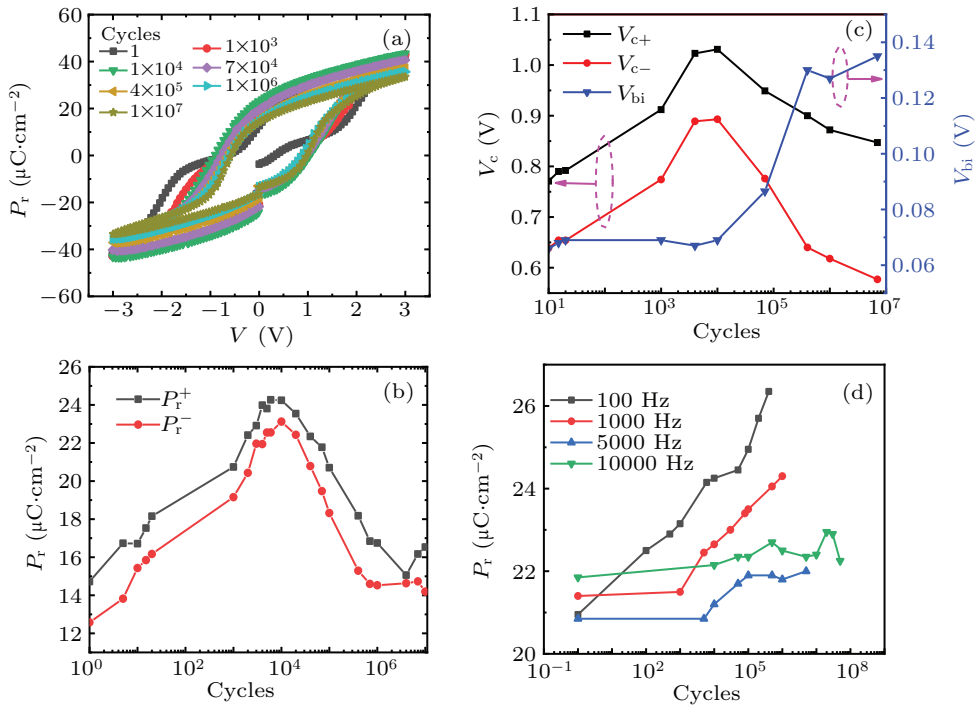


Fig. 1. Changes in (a) P–V hysteresis loops, (b) remnant polarization, (c) coercive voltage and built-in voltage with switching cycles under 1-kHz square waves. (d) Changes in remnant polarization as a function of switching cycles under square waves with various frequencies.

The wake-up test was also performed under various frequencies, as shown in Fig. 1(d). As the switching frequency decreased, fewer switching cycles were needed to reach the same polarization increase relative to that from higher switching frequencies. This was consistent with previous results that a higher number of cycles was necessary to acquire the same remnant polarization at higher wake-up frequencies.[13]

The dominant conduction mechanism for the HZO thin film was analyzed. It was firstly polarized with +3 V to preset the polarization state. Then the I–V curve was measured in the $0 \rightarrow 3$ V region, as illustrated in Fig. 2(a) with a double-logarithmic scale. As the voltage increased, the I–V curve exhibited a linear behavior (slope k of 1.1) at low voltage (< 0.6 V), and then a quadratic behavior ($k = 2.2$) at higher voltage. At 1.7 V, the current rose sharply and the slope was 6.9. The conduction behavior was consistent with trap-controlled space-charge-limited (SCL) conduction,[22–24] with three regions corresponding to Ohmic, SCL, and trap-filled-

limited conduction.[25] The origin of the space charges in the ferroelectric material is related to oxygen vacancies. They create trap energy levels in the bandgap for activated electrons to be mobile.[22] Thus, it is reasonable to assign oxygen vacancies as the physical origins for the traps in the film. Figure 2(b) displays the *I*–*V* curves for various numbers of switching cycles. It reveals that both the linear part (Ohmic conduction) and the SCL current remained stable up to 10^5 cycles, indicating that the number of charge carriers associated with oxygen vacancies did not change in the wake-up process. This was consistent with previous results that no oxygen vacancies were generated in the wake-up stage.[12]

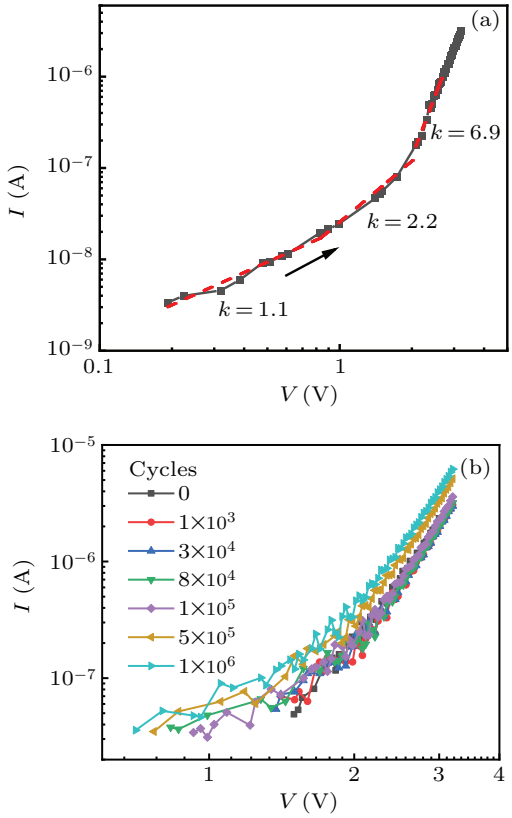


Fig. 2. (a) The *I*–*V* characteristics under positive bias. The arrow denotes the sweep direction. (b) Changes in *I*–*V* curves with respect to switching cycles.

The device was also repetitively switched with 1-kHz, ±3 V pulsed waveforms. The pulse width ranged over 0.01–0.5 ms. It can be seen from Fig. 3(a) that when the pulse width was less than 0.1 ms, the polarization did not exhibit a wake-up effect. Only when the pulse width was a certain length did the wake-up appear, which implied that the voltage application time in each switching cycle was an important factor. We plotted the remnant polarization over the total duration of the applied field for both square and pulsed waves in Fig. 3(b). The longer voltage application times in each cycle resulted in a faster wake-up. Furthermore, a wake-up also occurred when a DC voltage was applied. In Fig. 3(b), the rise of remnant polarization under continuous DC voltage was close to that from the cycling wake-up for the equivalent duration. Hence, we can explain the wake-up effect in terms of the redistribution of oxygen vacancies, although there is no generation of new $V_{Ö}$ at this stage. The positively charged oxygen vacancies moved under the external electric field. When the application time of each voltage cycle did not reach a certain limit, the vacancies just vibrated in their original positions and did not change their distribution. When the application time was sufficiently long, the $V_{Ö}$ left their initial positions, resulting in a net migration and redistribution that contributed to the wake-up process. In that case, both the voltage application time in each cycle and the cumulative electric field duration affected the wake-up process.

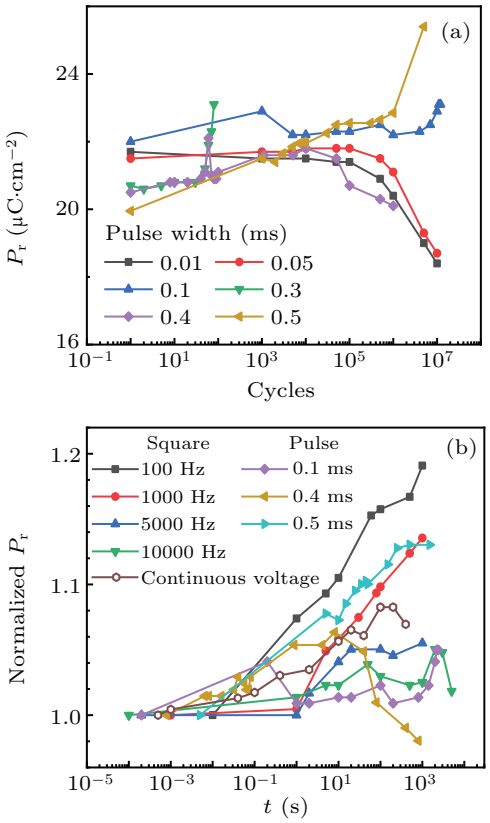


Fig. 3. (a) Change in remnant polarization as a function of switching cycles under 1-kHz waves with various pulse widths. (b) Normalized change in P_r over the duration of the switching electrical field for both square (#cycles/frequency) and pulse waveforms (#cycles×pulse width×2). The results are compared with the rise of P_r under a continuous DC electric field.

For further verification, *C*–*V* loops were measured for the cycled samples. In Fig. 4(a), the capacitance decreased with the increasing number of electric field cycles. Lomenzo *et al.*[26,27] suggested that the decreased dielectric constant in the wake-up state was caused by the tetragonal-to-ferroelectric orthorhombic phase transition. Pintilie *et al.* proposed that the *C*–*V* curve of a ferroelectric material can be expressed by[17,28]

$$C = \sqrt{\frac{q\varepsilon_0\varepsilon_s N_{\text{eff}}}{2(V + V_{\text{bi}} \pm \frac{P}{\varepsilon_0\varepsilon_s}\delta)}}, \tag{1}$$

where $N_{\rm eff}$ is the effective charge density in the space-charge region of the Schottky diode, $V_{\rm bi}$ is the built-in potential in the absence of polarization, δ is the distance between the polarization sheet of charge and the physical metal–ferroelectric interface, q is the carrier charge, ε_0 is the permittivity of free space, and $\varepsilon_{\rm s}$ is the static dielectric constant. The $\pm$ sign indicates two possible orientations of polarization P. The C–V curve in the area enclosed by the green dashed line in Fig. 4(a) was chosen and the corresponding slope of $1/C^2$–V was fit to extract $N_{\rm eff}$ for the interface under reverse bias. The inset in Fig. 4(b) displays the linear fit of such a relationship to derive the initial charge density near the top electrode/film interface. The dependence of $N_{\rm eff}$ on switching cycles is illustrated in Fig. 4(b) for the top and bottom interfaces.

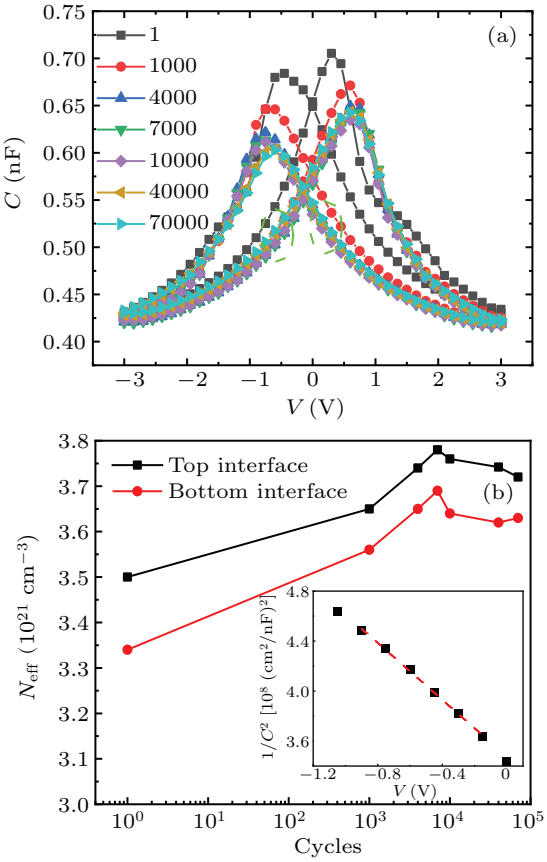


Fig. 4. (a) Change in C–V characteristics for the HZO thin film with various switching cycles. (b) Change in free-carrier concentration at both top and bottom electrode/film interfaces with respect to the switching cycles. The inset shows the $1/C^2$–V plot of the initial sample.

It shows that the effective charge density at the interfaces increased during wake-up. This could also be understood in terms of oxygen vacancy migration which is shown in Figs. 5(a)–5(c). Because the $V_{\ddot{O}}$ with positive charges can attract electrons, they usually act as electron-trapping centers.[17] Initially, the $V_{\ddot{O}}$ accumulated at the TiN/HZO interface (Fig. 5(a)), where a large number of electrons were needed to fill traps, causing a small density of free charge in the space-charge region. As the wake-up process continued during the initial 10^4 cycles, the oxygen vacancies moved away from the interface and went into the bulk of the HZO film as shown in Fig. 5(b), reducing the amount of $V_{\ddot{O}}$ at the interface. Therefore, the charged-carrier trapping was reduced, which resulted in an increased effective charge density at the interfacial space-charge region. It can also be derived that there should be a higher concentration of $V_{\ddot{O}}$ at the bottom interface than that at the top interface from the comparison of $N_{\rm eff}$ between the two interface as shown in Fig. 4(b). This gave rise to an upward built-in voltage[29] consistent with the result shown in Fig. 1(c). After the wake-up stage, the film was fatigued to have an obvious reduction in polarization. On the basis of the long-term study of fatigue mechanism, the fatigue behavior is considered to be closely related to the generation of oxygen vacancies in the film.[30,31] The increase of oxygen vacancies caused the reduction of effective charge density after 10^4 cycles as shown in Fig. 4(b). It is possible that the difference between the concentration of $V_{\ddot{O}}$ at the top and bottom interface became larger (Fig. 5(c)). As a result, the built-in voltage increased rapidly in the fatigue process as displayed in Fig. 1(c). However, the scenario requires for more investigation in future work.

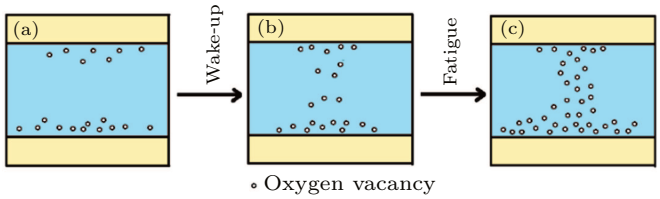


Fig. 5. Schematic of the migration and generation of oxygen vacancies from (a) initial → (b) wake-up → (c) fatigue state under the repetitive switching process. The hollow circles represent the oxygen vacancies.

4. Conclusions

The wake-up effect in the TiN/$Hf_{0.4}Zr_{0.6}O_2$/TiN structure was examined with various electrical cycling conditions. The total duration and the single length of an applied electrical field both affected the increased polarization. The current–voltage characteristics were consistent with space-charge-limited conduction. Both the stable Ohmic and SCL currents in the wake-up process indicated that the trap density in the film did not change during this period. The effective density of charge in the space-charge region demonstrated a decreased trap density at the interface. Considering the important role of oxygen vacancies as trap centers and their migration under an electric field, the wake-up effect and other property changes were attributed to the redistribution of oxygen vacancies.

Acknowledgements

Project supported by the National Natural Science Foundation of China (Grant No. 61201046) and the Natural Science Foundation of Beijing, China (Grant Nos. 4202009 and 4162013).

References

[1] Böscke T S, Mäller J, Bräuhaus D, Schröder U, Böttger U, Sundqvist J, Kücher P, Mikolajick T and Frey L 2011 *Appl. Phys. Lett.* **99** 102903

[2] Sang X H, Grimley E D, Schenk T, Schroeder U and LeBeau J M 2015 *Appl. Phys. Lett.* **106** 162905

[3] Fan Z, Chen J S and Wang J 2016 *J. Adv. Diele.* **6** 1630003

[4] Zhao W, Fu Z Q, Deng J M, Li S, Han Y F, Li M R, Wang X Y and Hong J W 2021 *Chin. Phys. Lett.* **38** 037701

[5] Wang J L, Wang D, Li Q, Zhang A H, Gao D, Guo M, Feng J J, Fan Z, Chen D Y, Qin M H, Zeng M, Gao X S, Zhou G F, Lu X B and Liu J M 2019 *IEEE Electron Dev. Lett.* **40** 1937

[6] Tang H, Tang X G, Jiang Y P, Liu Q X and Li W H 2019 *Acta Phys. Sin.* **68** 227701 (in Chinese)

[7] Jia Z, Ren T L and Zhang Z G 2006 *Chin. Phys. Lett.* **23** 1943

[8] Wen X Y, Yu J, Wang Y B, Zhou W L, Gao J X and Chu X H 2008 *Chin. Phys. Lett.* **25** 2694

[9] Yang Y, Zhou C J, Peng P G, Xie D, Ren T L, Pan X and Liu J S 2012 *Chin. Phys. Lett.* **29** 128501

[10] Wu Q, Wu X, Zhao Y S and Zhao S F 2020 *Chin. Phys. Lett.* **37** 118401

[11] Ali T, Polakowski P, Riedel S, Büttner T, Kämpfe T, Rudolph M, Pätzold B, Seidel K, Löhr D, Hoffmann R, Czernohorsky M, Kühnel K, Steinke P, Calvo J, Zimmermann K and Müller J 2018 *Appl. Phys. Lett.* **112** 222903

[12] Pešić M, Fengler F P G, Larcher L, Padovani A, Schenk T, Grimley E D, Sang X, LeBeau J M, Slesazeck S, Schroeder U and Mikolajick T 2016 *Adv. Funct. Mater.* **26** 4601

[13] Starschich S, Menzel S and Böttger U 2016 *Appl. Phys. Lett.* **108** 032903

[14] Park M H, Kim H J, Kim Y J, Lee Y H, Moon T, Kim K D, Hyun S D and Hwang C S 2015 *Appl. Phys. Lett.* **107** 192907

[15] Zhou B H, Zhang F J, Liu X, Song Y and Zuo X 2020 *Chin. Phys. B* **29** 047103

[16] Wang Z C, Cui Z Z, Xu H, Zhai X F and Lu Y L 2019 *Chin. Phys. B* **28** 087303

[17] Yang Y, Zhu H, Chu D P, Liu K, Zhang Y L, Pei M H, Feng S W, Jin L, Wang C, Liu J, Li R and Wang S 2020 *J. Phys. D* **53** 115301

[18] Zhao J J, Zhang J S, Zhang F, Wang W, He H R, Cai W Y and Wang J 2019 *Chin. Phys. B* **28** 126801

[19] Chen M C and Jiang A Q 2011 *Chin. Phys. Lett.* **28** 077701

[20] Zhu L, Zhu X L, Liu X Q and Chen X M 2021 *Chin. Phys. Lett.* **38** 047701

[21] Lichtensteiger C, Weymann C, Fernandez-Pena S, Paruch P and Triscone J 2016 *New J. Phys.* **18** 043030

[22] Zhu H, Yang Y, Meng X, Jiang A Q, Bai Z L, Zheng X, Jin L, Wang C and Feng S W 2018 *Appl. Phys. Lett.* **112** 182904

[23] Shang D S, Wang Q, Chen L D, Dong R, Li X M and Zhang W Q 2006 *Phys. Rev. B* **73** 245427

[24] Chen X M, Wu G H, Zhang H L, Qin N, Wang T, Wang F F, Shi W Z and Bao D H 2010 *Appl. Phys. A* **100** 987

[25] Zhu H, Zhang Y Q, Jiang A Q, Bai Z L, Feng S W, Wang P F, Meng X and Qi Q 2016 *Appl. Phys. Lett.* **109** 252901

[26] Lomenzo P D, Takmeel Q and Zhou C Z 2015 *J. Appl. Phys.* **117** 134105

[27] Pintilie L, Stancu V, Trupina L and Pintilie I 2010 *Phys. Rev. B* **82** 085319

[28] Pintilie L and Alexe M 2005 *J. Appl. Phys.* **98** 124103

[29] Lo V C 2002 *J. Appl. Phys.* **92** 6778

[30] Desu S B and Yoo I K 1993 *Integrated Ferroelectr.* **3** 365

[31] Chen M, Liu Z L, Wang Y and Yao K L 2005 *Phys. Status Solidi A* **202** 1166